

An investigation of IBM Quantum Computing device performance on Combinatorial Optimisation Problems

Maxine T. Khumalo · Hazel A. Chieza · Krupa Prag · Matthew Woolway

Dated: 8 July 2021

Abstract The exponential increase in CPU time taken to deterministically solve \mathcal{NP} -Hard Combinatorial Optimisation Problems (COP), as the problem size scales, has resulted in a search for non-deterministic optimisation solution techniques to obtain solutions to COP efficiently. This paper juxtaposes classical and quantum optimisation algorithms' performance to solve two common COP, the Travelling Salesman Problem (TSP) and Quadratic Assignment Problem (QAP). The two classical optimisation techniques applied are Branch and Bound (BNB) and Simulated Annealing (SA), and the two quantum optimisation methods used are the Variational Quantum Eigensolver (VQE) algorithm and Quantum Approximate Optimisation Algorithm (QAOA). These algorithms are respectively executed on classical and IBM's suite of Noisy Intermediate-Scale Quantum (NISQ) computers. Our experimental results resemble and extend on previously reported results in the litera-

Maxine T. Khumalo
 University of the Witwatersrand
 School of Computer Science and Applied Mathematics
 E-mail: 1604282@students.wits.ac.za

Hazel A. Chieza
 University of the Witwatersrand
 School of Computer Science and Applied Mathematics
 E-mail: 1609247@students.wits.ac.za

✉ Krupa Prag
 University of the Witwatersrand
 School of Computer Science and Applied Mathematics
 E-mail: krupa.prag@wits.ac.za

Matthew Woolway
 Imperial College London
 Department of Mathematics
 E-mail: m.woolway@imperial.ac.uk
 University of Johannesburg
 Faculty of Engineering and the Built Environment
 E-mail: mjwoolway@uj.ac.za

ture. Extensions include critically analysing, comparing and commenting on the performance of quantum optimisation computing techniques to classical techniques, with respect to computational time and additional metrics used to measure solution quality. Furthermore, a comparison of the impact of a new set of basis gates on the quantum optimisation techniques was investigated; the results did not reflect any consistent impact on results. The VQE algorithm and QAOA executed on state of the art IBM quantum devices are outperformed by classical optimisation techniques, highlighting the shortcomings of NISQ devices.

Keywords Quantum Computing · IBM Qiskit · Optimisation · TSP · QAP · VQE · QAOA

1 Introduction

Two important examples of \mathcal{NP} -Hard Combinatorial Optimisation Problems (COP) are the Travelling Salesman Problem (TSP) and Quadratic Assignment Problem (QAP). The TSP requires finding the shortest route to visit all enlisted locations [12], while the QAP aims to find the minimum cost of allocating facilities to locations [28]. Both TSP and QAP can be translated to solve numerous industry challenges. Common TSP real-world applications found in the literature include X-ray crystallography [6], computer wiring [32], and various routing and scheduling problems [13, 30]. Similarly, some use cases of the QAP formulation include energy system problems [2], backboard wiring [7], typewriter keyboard design [8], the hospital layout challenge [17], and campus building arrangement [15].

Solutions to these combinatorial problems have been extensively studied using various optimisation techniques

implemented on classical devices [30, 7]. However, recent advances in Quantum technology have led to the investigation of these quantum devices' performance when applied to various COP instances. Specifically, through the use of Noisy Intermediate-Scale Quantum (NISQ) technology, preliminary findings for both the TSP [51, 45] and QAP [2] have been reported. A detailed and comparative investigation into the performance of the Variational Quantum Eigensolver (VQE) algorithm run on these NISQ devices against classical devices [9] showed the classical optimisation techniques significantly outperform the suite of IBM devices utilised.

In this paper, we extend the state-of-the-art benchmarks reported in [9] by including the newest and largest current IBM devices available. We further introduce preliminary findings for the Quantum Approximate Optimisation Algorithm (QAOA) on amenable tractable problem instances. Additionally, we present a feasibility metric and new metric to determine the spectrum of the feasibility of quantum algorithms on the ensemble of IBM devices. Finally, we investigate the computational performance improvements by utilising the *conditional reset* feature on the IBM systems over those used in [9].

The remainder of the paper is organised as follows. Section 2 presents the complexity classification and the formulation of the TSP and QAP. Section 3 discusses the techniques and algorithms used for both the classical and Quantum devices. Section 4 details the experimental procedure and settings used in conducting the experiments. Results and analysis are presented in Section 5, with conclusions drawn in Section 6.

2 Background

The TSP has been extensively studied and reviewed. Seminal research of the TSP occurred in 1959 with the Dantzig-Fulkerson-Johnson (DFJ) [12] formulation, detailing how the TSP problem instances of up to 52 locations could be solved using an exact algorithm. The DFJ formulates the TSP as an Integer Linear programming (ILP) and then utilises an exact cutting-plane algorithm to solve the LP relaxation of the ILP. The TSP forms the basis of many complex COP that model the intricacies of real-world scenarios. The complexity class of the TSP is \mathcal{NP} -Hard [1], which makes it intractable to exactly solve the problem using deterministic algorithms as the problem size scales. Therefore, research developments of the TSP have turned the focus on non-deterministic heuristic and meta-heuristic methods. One of the most effective heuristics in the literature is the Lin-Kernighan (LK) algorithm [33], which utilises an adaptive algorithm that consists of

swapping the edges of sub-tours to create a new tour with an overall minimal distance. Other notable heuristics and meta-heuristic algorithms which have applied to the TSP include; the Simulated Annealing (SA) algorithm [27], Gene Expression Programming [21], and the Ant Colony Optimisation algorithm [16]. These algorithms perform well in the literature, and on-going research is often an extension, adaptation or combination of these fundamental and well-known algorithms [55].

The QAP was first formulated by Koopmans and Beckmann (1957) [28]. It found importance due to the added relative cost of assignment with a quadratic objective function to solve assignment class problems, a phenomenon prevalent in industry [28]. Practically, the QAP is primarily solved via heuristics as similar to the TSP; the problem becomes intractable as the problem instances scale in size. The QAPLIB documents a set of QAP benchmark problems and their best solutions as reported in the literature. QAPLIB records the following methods as most effective on large instances of the QAP: Branch and Bound [31], Tabu Search [48] and Ant Colony Optimisation [16, 47].

Using quantum computing methods to solve the TSP and the QAP begins with Computational Complexity Theory. As previously mentioned, the TSP and the QAP are both \mathcal{NP} -hard problems [1, 44], which means that as the problem scales in size, it becomes difficult for a classical computer to find an optimal solution in polynomial time [7]. Quantum Complexity Theory describes the computational complexity of quantum computers. Quantum Complexity Theory is necessary because there are problems too complex to solve with classical computing methods that quantum computers can theoretically solve [5] and these problems computational complexity requires description. Between a classical probabilistic Turing machine and a Quantum Turing Machine (QTM), a polynomial-time QTM is more powerful in certain search algorithms [4, 5, 14]. A basic search algorithm for optimisation problems has complexity $\mathcal{O}(2^n)$ on a classical computer while a quantum search algorithm for an \mathcal{NP} -Complete problem reduces this to complexity $\mathcal{O}(\sqrt{n})$ [24, 38, 43]. Therefore, there is reason to believe that there may be a speed-up from quantum computing when applied to optimisation problems.

2.1 Mathematical Model

2.1.1 Travelling Salesman Problem

The TSP has multiple mathematical formulations [1], however, the DFJ formulation [12] has the ability to

form a strong LP relaxation which makes it the preferred formulation of the TSP. This formulation is given as follows:

$$\min \sum_{i=1}^n \sum_{j=1}^n d_{ij} x_{ij} \quad (1)$$

Subject to:

$$\sum_{j=1}^n x_{ij} = 1, \quad i = 1, \dots, n, \quad (2)$$

$$\sum_{i=1}^n x_{ij} = 1, \quad j = 1, \dots, n, \quad (3)$$

$$\sum_{i,j \in S} x_{ij} \leq |S| - 1, \quad (4)$$

$$S \subset V, 2 \leq |S| \leq n - 2, \quad (5)$$

$$x_{ij} \in \{0, 1\}, \quad (6)$$

$$i, j = 1, \dots, n \quad i \neq j. \quad (7)$$

Equation (1) is the objective function that seeks to minimise the total travelled distance, subject to constraints (2-7). The distance between city i and city j can be denoted in the form of a distance matrix by d_{ij} . The binary decision variable, x_{ij} , indicates whether a path between cities i and j exists.

Constraint (2) and constraint (3) prevent any city from being visited more than once. The sub-tour elimination constraints (4) and constraint (5) ensure that all cities of a TSP problem are visited, where S is a subset of the n cities. Because the sub-tour-elimination constraints' variables grow exponentially, it is intractable to directly solve the DFJ formulation. For every value of n , there is $2^n - 2n - 2$ sub-tour-elimination constraints and $n(n - 1)$ binary decision variables.

2.1.2 Quadratic Assignment Problem

To mathematically model the QAP, weights are defined for the cost associated with moving goods between location k and l (b_{kl}) and factories k and l (c_{kl}) [28]. The cost function is then calculated by finding the product of the associating costs of allocated factories to locations. This allocation is denoted by a permutation function π that records which factories are allocated to which locations. The elements in π are the factory number allocated to the location represented by its position in the vector. The QAP objective function is:

$$\min \sum_{k=1}^n \sum_{l=1}^n b_{kl} c_{\pi(k), \pi(l)}, \quad (8)$$

where b and c are matrices of dimensions $n \times n$ [7]. The full form of the objective function is:

$$\sum_{k=1}^n \sum_{l=1}^n b_{kl} c_{\pi(k), \pi(l)} + \sum_{k=0}^n a_{k, \pi(k)}, \quad (9)$$

where the value a_{kl} represents the cost of allocating factory k to factory l is known as the “cost of assignment”. This additional cost term is omitted in the benchmark formulations for ease of calculation [7].

The QAP is a quadratic optimisation problem because of its quadratic objective function. The QAP is also a bijection of a finite set \mathcal{N} because unique position values from set \mathcal{N} are allocated as elements of π [7]. This characteristic means that the QAP can have a “0-1” integer optimisation problem formulation [7, 31]. This “0-1” integer formulation is the version used to solve the QAP with quantum computing.

2.1.3 Quantum formulations

To apply quantum algorithms to find solutions of COP problems using a quantum devices, the problems' objective function first needs to be mapped to a Hamiltonian form [3]. The respective Hamiltonian of Ising model formulation mappings of the TSP and QAP, described in Section 2, are presented in this section.

The objective and constraints of the TSP can be described by:

$$\sum_{i,j} d_{ij} \sum_p x_{ip} x_{jp+1} + A \sum_p \left(1 - \sum_i x_{ip} \right)^2 + A \sum_i \left(1 - \sum_p x_{ip} \right)^2. \quad (10)$$

Similarly, the QAP can be described by:

$$\sum_{m=1}^n \sum_{u=1}^n \sum_{k=1}^n \sum_{l=1}^n C_{lk} T_{um} x_{ul} x_{mk} + B \sum_l \left(1 - \sum_u x_{ul} \right)^2 + B \sum_u \left(1 - \sum_l x_{ul} \right)^2, \quad (11)$$

by assigning

$$x_{ip} \rightarrow (1 - Z_{ip})/2,$$

and

$$x_{ul} \rightarrow (1 - Z_{ul})/2,$$

where Z_{ij} is a Pauli operator that maps the TSP to a Hamiltonian, and Z_{ul} is a Pauli operator that maps the QAP to a Hamiltonian [3, 34, 2]. A and B are free parameters that satisfy the constraints. The VQE and QAOA algorithms are used to find the ground state of the respective Hamiltonian systems for the TSP and QAP, described by equation (10) and equation (11).

The ground state is where the expectation value of the energy state is the lowest. Both quantum algorithms, VQE and QAOA, applied to the TSP and QAP use variational methods which consist of selecting a variational form. This method depends on finding one or more parameters to find approximations to the ground state. Simply, this describes an ansatz in the form of a parametrised circuit. The accuracy of solutions depends on the variational form [37]. The depth of the variational form is the exponential to the number of qubits, hence the parameters of a variational form exponentially increase with the number of qubits. Due to the limited number of qubits currently available on NISQ devices, the size of the problem instances considered is restricted [42].

The VQE algorithm was proposed by [41] to approximate the ground state energy of a molecule [3] and early applications of VQE to chemistry problems were predominantly studied. Recently, the literature on the VQE applications has been extended to solve COP [37, 50]. Preliminary results using NISQ technology to find solutions to the QAP are shown in [2]. The VQE algorithm's performance is benchmarked against classical algorithms, SA and BNB, for the TSP and QAP in [9]. The findings in [9] show that the classical algorithms SA and BNB outperform the VQE algorithm with reference to both solution quality and computational time. This work aims to expand on [9], by introducing additional metrics to measure solution quality and comparing the results to the COPs obtained using the VQE algorithm to an additional quantum algorithm, QAOA. Recent developments on the QAOA are outlined in [56], and applications of the QAOA to solve the Maxcut, a prominent COP, have been investigated [11, 20, 25]. The literature on the QAOA includes studies to improve the QAOA using graph theory to optimise the solving of the Hamiltonian [50], and the p -value approach [18].

3 Solution Techniques

This section discusses classical and quantum techniques used to obtain solutions to the TSP and QAP.

3.1 Branch and Bound

The Branch and Bound (BNB) algorithm is an exact algorithm that reduces the computational runtime of obtaining a solution as it indirectly computes all possible combinations of a given COP [39]. The BNB first solved a discrete \mathcal{NP} -hard optimisation problem [29], namely the British Petroleum TSP problem. The BNB represents optimal and sub-optimal solutions in the form of

a tree data structure constructed with multiple levels of artificial nodes. Each node represents a calculated distance for the TSP [22], and an allocation permutation vector π and product of distance and flow for the QAP [10]. At each level, the node with the lowest value is further explored and broken into sub-problems. This iterative process is terminated when a complete tour is formed for the TSP, and a suitable permutation matrix is formed for the QAP. Nodes are selected to explore using the best-first strategy, which entails comparing the rolling cost function values between levels to explore further which nodes to explore. The efficiency of the BNB algorithm depends on an appropriate estimation of the lower bound. As a result, a suitable bound should first be calculated before implementing the BNB algorithm.

3.2 Simulated Annealing

SA is a stochastic optimisation technique for approximating the global optimum of a given objective function. This technique is based on the concept of annealing, which comes from metallurgy and statistical physics. Annealing is the idea of slowly cooling down a metal (initially at a high temperature) to ensure that the metal particles are orderly arranged to strengthen the metal [7]. SA was designed to solve COP [27]. The algorithm commences with an initial random solution and a high temperature. A cooling schedule controls the decrease of the temperature [27]. SA is built on the Metropolis Algorithm [26, 36] which is moderated by a decreasing temperature parameter. A slow decrease in the temperature allows SA to explore the search space irrespective of the quality of the solution. This decrease in the temperature helps to prevent local optimal solutions [49]. At each temperature, a neighbourhood search algorithm generates a solution. That updated solution's cost is compared to the rolling best solution. If the randomly generated solution is worse than the current best solution, the randomly generated solution becomes the new best solution. A Markov Chain is included in SA to moderate the temperature [49]. This process ends at "the ground state" (the lowest temperature value allowed), revealing the best solution found [52].

3.3 Variational Quantum Eigensolver

The VQE algorithm is a quantum-classical hybrid algorithm that has two components, a quantum sub-routine and a classical loop [41]. The VQE algorithm's objective is to find the ground state, or the minimum eigenvalue of the Hermitian matrix [3]. The Hermitian matrices are

suitable for describing the Hamiltonian H of quantum systems, which represents the total energy of a considered system. The Hamiltonian system of a given COP can be described by:

$$H = \sum_{\alpha} h_{\alpha} \otimes_{j=1}^N \sigma_{\alpha_j}^{(j)}, \quad (12)$$

where σ_{α} is the Pauli matrix acting in the Hilbert space, \otimes is a tensor product of Pauli matrices and h_{α} is the Hamiltonian coefficient. The VQE is an iterative algorithm used to find the lowest eigenstate of the Hamiltonian system. The output of the quantum subroutine is used to update the ansatz. The ansatz of the VQE algorithm, which is classically prepared, are the parameterised trial states $|\psi(\theta)\rangle$. The quantum subroutine calculates and returns the expectations of the energy of the provided ansatz or the measured Hamiltonian. The expectation value is measured such that it satisfies the variational principle, which states that the expectation value is always greater than or equal to the ground state of the system [41]. The Rayleigh-Ritz variational principle states:

$$\langle \psi(\vec{\theta}) | H | \psi(\vec{\theta}) \rangle \leq \langle \psi(\theta_0) | H | \psi(\theta_0) \rangle = E_0, \quad (13)$$

where $|\psi(\theta)\rangle$ is any parameterised trial state and E_0 is the ground state. This principle ensures that VQE converges to the lowest possible eigenstate [41].

The variational method is a robust method for quantum computing, as unlike modern classical computing or theoretical quantum computing, NISQ technology is susceptible to significant errors as a result of noise [3]. This noise is due to the sensitivity of qubits to the environment, and hardware limitations of hardware [40]. However, even with accounting for noise, the VQE algorithm's solutions will not overshoot the minimum, provided the ansatz of $\vec{\theta}$ includes the ground state [37]. This is an advantage that makes the black-box optimiser, VQE, robust to noise.

Classical algorithms are applied to minimise the measured Hamiltonian state's expectation value by updating the parameter values. This occurs within the classical loop by finding the optimal set of θ parameters. Qiskit has an array of optimisers available, including COBYLA, LBRFGS and RBTOpt. The optimiser selected is based on the VQE circuit's depth, which is to be executed [3]. The VQE is a variational algorithm that favours short-depth circuits, which can be executed on NISQ devices [42]. However, the VQE's heuristic nature does not guarantee the global optimal solution [37]. The VQE algorithm's performance depends on the variational form, a classical optimiser and the number of shots for each experiment. The variational form is the initial circuit that approximately determines the

ground state of the Hamiltonian system. The type of circuits options available, on Qiskit, to represent the variational form are: TwoLOCAL (TL) circuit (linearly entangled, with an RY-gate layer) and the REALAMPLITUDES (RA) circuit (linear entanglement). A disadvantage of variational algorithms implemented on gate-model quantum computers like IBM's, is that they are predisposed to barren plateaus. Barren plateaus are where the gradient of the objective function exponentially decreases as a function of the number of qubits [23]. These occur when using classical gradient descent methods and there is no change in objective value [35]. A large circuit's average value of the gradient of the objective function is zero in barren plateaus, which means a solution cannot be obtained [23].

3.4 Quantum Approximate Optimisation Algorithm

The Quantum Approximate on Algorithm (QAOA) was introduced by [19] and, like the VQE, is based on the Variational Principle but has a unique trial state selection. Where VQE chooses a generic trial function $|\psi(\theta)\rangle$, the QAOA uses a Hamiltonian to build the trial function [53]. A Hamiltonian is used to described a cost function $C(x)$. The QAOA begins by finding a trial state $|\psi_p(\gamma, \beta)\rangle$ with real parameters γ and β such that the expectation value of the Hamiltonian is satisfied,

$$\min F_p(\gamma, \beta) = \langle \psi_p(\gamma, \beta) | H | \psi_p(\gamma, \beta) \rangle \quad (14)$$

The trial state that depends on the parameters γ and β , is prepared on a quantum computer and measured in the computational basis. Then a bit string x^n is obtained. Continuous repetition of this process using the same value of γ and β will produce an optimal bit string x^* . This bit string, when measured in the computational basis, can be shown to have a high probability of minimising the cost function $C(x^*)$. The integer, p , determines the circuit's depth level where each trial state is prepared. The depth level of the circuit is described by p where $p \geq 1$ and the accuracy of the QAOA is said to improve as p increases [56]. Unlike VQE, QAOA has no initial variational form [3]. Therefore, QAOA is less configured, making it potentially more effective at converging. QAOA using quantum computers to prepare parameters means it uses more quantum functions and exposes the results to more error [3, 46].

3.5 New Set of Basis Gate on IBM Quantum Devices

Quantum algorithms are often graphically represented as quantum circuits in the literature [25]. Logic gates are used to describe the computational operations which

Table 1: Description of the IBM Basis Gates

IBM Devices' Gates	Description
Controlled NOT gate (CX)	Creates entanglement if target qubit is in superposition
Identity gate (ID)	No operation is performed on a qubit
RZ	Rotation of qubit state around z axis
Square Root of X gate (SX)	Creates superposition on qubit in downstate
X	Changes state of qubit from down state to up state and vice versa

change a state of a qubit in a quantum circuit [3,54]. Some of the most common and basic quantum gates are the Hadamard gate and the Controlled NOT (CX) gate. The new set of basis gates on the IBM quantum devices currently consist of the (CX, ID, RZ, SX, X); these recently changed from (CX, ID, U1, U2, U3) the original set of basis gates [3]. The recent change to the IBM quantum gates is a conditional reset. The conditional reset feature initialises qubits in the $|0\rangle$ state through measuring, followed by a conditional NOT (CNOT) gate. Conditional reset allows faster circuit execution by reducing the initialisation time between shots - i.e. we would predict a decrease in computation time. Conditional reset also allows qubit reuse for circuits requiring a source of “fresh ancillas”. Ancillas moderate the interaction of qubits in a quantum register. Qubit reuse should make calculating circuits more efficient. IBM implemented state-discrimination logic in control systems to decode qubit states from received microwave pulses. Over $1\ \mu\text{s}$, the control identifies the qubit states and executes the qubit reuse. Enabling hardware state discrimination negates the necessity for discrimination calibration circuits (these were previously attached to each job). It therefore can be predicted that the conditional reset should improve the quality of results on the metrics investigated.

4 Methodology

4.1 Experimental Settings

An Intel® Core™ i5-6200U CPU @ 2.30GHz 4GB 64 bit Microsoft Windows 10 operating system was used to obtain the classic results on Python 3.6.5. Quantum algorithms are from the Aqua library on the open-source Python framework - Qiskit. The IBM Quantum Experience Cloud was used to run all quantum experiments across various IBM simulators and quantum devices. The latest Qiskit version (0.23.3) allows access to devices with improved operational gates; however, to compare the performance of IBM quantum hardware on COP, an older version of Qiskit (0.20.0), in addition

to the new version, was used. The programme for all experiments can be found on Github.

4.1.1 Algorithm Implementation

The Qiskit framework has a library called Qiskit Aqua that supports quantum algorithms like the VQE and QAOA. The parameters associated with the VQE and QAOA have different functions that affect their overall performance when applied to a COP. The variational form is one such parameter. This parameter approximates a circuit that determines the ground state of a Hamiltonian system. The TwoLOCAL and REALAMPLITUDE circuits were used in this research for the VQE. Unlike the VQE, where a variational form can be configured, the QAOA develops its own variational form. The Qiskit variational form for the QAOA depends on a p -value, which determines the parametrised circuit’s depth. To increase optimality, a p -value of 3 is set for the QAOA on both the TSP and QAP. The number of shots, which provides a distribution of the results, is another parameter that affects the VQE and QAOA performance. The default number of shots for the VQE and QAOA is set at 1024 and 8192 respectively. Considering that the expectation value of a quantum state is optimised through classical optimisers, the Simultaneous Perturbation Stochastic Algorithm (SPSA) is recommended for variational quantum algorithms [3]. Because of the various states that occur with probability, the state with the most probable feasible solution is chosen as the final solution. For the quantum experiments, a simulator, using the Matrix Product State (MPS), was used to find a good enough initial point that was used on the actual quantum devices. The MPS method uses a compact form to formulate two-qubit gate operations which implement the VQE [3]. The strength of the initial point results in an estimation of solutions that are in the neighbourhood of the optimal solution and provides a higher probability of converging to the optimal solution, this is especially true for the VQE [37]. Classical simulators do not experience as much noise compared to actual quantum devices hence obtaining an initial point through the simulators will increase the performance of

the quantum algorithms when applied to actual quantum devices. These quantum devices (seen in Table 2) are limited to the number of qubits they support (i.e n cities/locations uses n^2 qubits) as well as the depth of a circuit.

Using Discrete Optimisation CPLEX (DOcplex), the “0-1” integer formulation of the QAP can be converted into a Quadratic Program. The Quadratic Program model can easily be mapped to a Hamiltonian using a Qiskit module. The “0-1” integer formulation for the TSP is directly mapped to a Hamiltonian using a Qiskit module. The BUILDMODEL function in Algorithms 1 and 2 represents these processes of building a Hamiltonian. The Variational Quantum Eigensolver (VQE) consists of three functions. The first is the fitness function using the “0-1” formulation of the QAP. The following function is a feasibility verifier where the permutation matrix x is checked against the constraints of the integer formulation of the QAP (a facility can only be assigned to one location and vice versa). Thirdly, the VQE has a function that returns all the feasible solution eigenstates and their accompanying probabilities. Since the VQE returns a distribution of probabilities for a suite of solutions, this function lists the returned eigenstates that are feasible along with their associated probability. This last function is called FEASIBLEOUTPUT in Algorithm 1. When using quantum computers as the backend, they are accessed through an IBM account, and the commands and results are sent via the internet. Algorithm 1 shows the implementation of VQE.

Algorithm 1 Variational Quantum Eigensolver (VQE)

Input:
 1: `inputmatrix(ces), circ, initialpoint, maxiter`
Output:
 2: $\pi^*, cost^*$
 3: initialisation;
 4: `qubit0pdocplex = BUILDMODEL(inputmatrix(ces))`
 5: `num = number of qubits of qubit0pdocplex`
 6: `spsa = SPSA(maxiter)`
 7: **if** `circ = RA` **then**
 8: `ry = REALAMPLITUDES(un, entanglement=linear)`
 9: **else if** `circ = TL` **then**
 10: `ry = TWOLOCAL(num, entanglement=linear)`
 11: **end if**
 12: `vqe = VQE(qubit0pdocplex, ry, spsa, initialpoint)`
 13: `quantuminstance = BACKEND(1024 shots)`
 14: `result = RUN(vqe, quantuminstance)`
 15: $\pi^*, cost^* = \text{FEASIBLEOUTPUT(result[eigenstate])}$

Algorithm 2 Quantum Alternating Optimisation Ansatz (QAOA)

Input:

1: `inputmatrix(ces), initialpoint, maxiter`
Output:
 2: $\pi^*, cost^*$
 3: initialisation;
 4: `qubit0pdocplex = BUILDMODEL(inputmatrix(ces))`
 5: `num = number of qubits of qubit0pdocplex`
 6: `spsa = SPSA(maxiter)`
 7: `qaoa = QAOA(qubit0pdocplex, spsa, initialpoint)`
 8: `quantuminstance = BACKEND(1024 shots)`
 9: `result = RUN(qaoa, quantuminstance)`
 10: $\pi^*, cost^* = \text{FEASIBLEOUTPUT(result[eigenstate])}$

4.2 Metrics

CPU time is used to measure the solution quality of the deterministic BNB algorithm used on the TSP and QAP. The stochastic nature of heuristic algorithms expands the number of performance measures that can test solution quality. At each experiment, 30 trials are executed and two success rates (SR) and a feasibility percentage are recorded. The SR metric describes the percentage amount of the trials within 95% and 99% of the optimal global solution. The feasibility percentage details the percentage of trials that generate a feasible solution. This paper will also look into a metric that is specific to quantum results. As briefly mentioned in Section 3.3, the number of shots details the number of times a quantum algorithm is repeated. By default, the number of shots was set to 1024 for the VQE and QAOA. This implies that a quantum algorithm is repeated as many times as the shots for any particular instance. This leads to a distribution of all the results obtained for that specific instance. The optimal solution for a particular trial is the most probable feasible quantum eigenstate in that distribution. This paper expands that idea introduced in [9] by considering a new metric called the *uncertainty percentage*. This uncertainty percentage tests the quantum solution’s quality by looking at how likely it is that solution can be obtained. An uncertainty percentage is calculated for each feasible solution in a set of 30 trials. This uncertainty percentage is based on the frequency of the quantum eigenstate. The uncertainty percentage analysis includes the average probability from the set, the maximum and minimum probability rates, and the standard deviation (note the headings in Table 6). In addition to the SR, feasibility rate and uncertainty percentage, the average CPU time is computed. IBM quantum devices are subject to calibration where a device is taken offline for performance testing. This does affect the CPU time on

Table 2: Specifications of the IBM Quantum Devices

Quantum Device	Version	Available Qubits	Max Shots	Max Circuits	Processor Type	Average Readout Error	Average CNOT Error
ibmq-johannesburg	1.2.2	20	8192	900	Penguin R3	8.412e-2	-
ibmq-boeblingen	1.2.9	20	8192	900	Penguin R4	5.258e-2	-
ibmq-montreal	1.9.7	27	8192	900	Falcon R4	2.067e-2	1.010e-2
ibmq-cambridge	1.2.0	27	8192	900	Falcon R1.1	12.682e-2	-
ibmq-sydney	1.0.37	27	8192	900	Falcon R4	3.876e-2	1.291e-2
ibmq-toronto	1.4.22	27	8192	900	Falcon R4	4.253e-2	1.157e-2
ibmq-rochester	1.2.0	53	8192	75	Hummingbird R1	14.448e-2	-
ibmq-manhattan	1.19.1	65	8192	900	Hummingbird R2	3.843e-2	1.541e-2

Omitted Average CNOT Error values of decommissioned IBM quantum devices. Further details of these devices can be found here.

a device for any particular experiment. As a result, two types of CPU time performances are being recorded - the average CPU time with outliers (AT) and the average CPU time without outliers (MT).

5 Results

The performance of the quantum optimisation algorithms benchmarked against classical optimisation algorithms, presented in Table 4, 5 and 6, and Figures 2, 3 and 1, are analysed with respect to both solution quality and computational time performance in this section.

The experimental results show that classical optimisation algorithms outperform quantum optimisation algorithms with respect to success rate, feasibility and computational time in finding solutions to the TSP and QAP.

The solution quality metrics results reported for problem instance of sizes 3 and 4 on the TSP and QAP suggest that the VQE performs better when compared with the QAOA. The solution quality metric results obtained for conditionally reset devices do not have a noticeable difference compared to the metrics of IBM devices that were not conditionally reset.

IBM has introduced the conditional reset feature in order to make the quantum device calculations more efficient. The results in Table 5 use the gates explained in Table 1 on the devices available with conditional reset on VQE and QAOA. Figure 1 compares the impact of conditional reset on time and for both average times AT and MT on both devices. From Figure 1, no clear improvement to computational time can be observed between results with or without conditional reset. When comparing the success rates in Table 5 to those on the same devices without conditional reset in Table 4, there is no improvement in success rate or feasibility. We, therefore, conclude that the implementation of conditional reset did not impact the results obtained.

Comparing the computational time taken to obtain a solution using classical algorithms in comparison to

the VQE algorithm, it was found that the applied classical algorithms had a faster computational time performance in comparison to the VQE algorithm. Figures 2 and 3 illustrate that the performance of the various employed quantum devices are consistent in terms of computational time, with the simulator performing the best. There is no distinct correlation between problem size and computational time for the quantum devices. However, this claim is made with a limited number of problem instances.

Success rate and feasibility are higher in SA than in VQE for most instances of the TSP and QAP, indicating that the SA obtains better solution quality than the VQE. From Table 4, it is evident the success rate and feasibility percentage decrease as the problem size increase. Instances of size 3 for the TSP applied to the VQE perform the best in terms of feasibility and success rate out of all the TSP instances. This is likely because the TSP has the least number of operations (Table 3). Instances of size 6 and 7 perform the worst with the most operations and largest parameters. `ibmq-qasm-simulator` has a higher feasibility percentage than the quantum devices. Comparing success rate and feasibility between devices shows no device has a superior performance to the others.

Comparing the results of the QAOA to those of VQE in Table 5, the QAOA takes a longer computational time performance on the quantum devices than the VQE. This increased computational time is likely due to increased operations and depth (Table 3). The success rate and feasibility of the QAOA are comparable to that of VQE. It is difficult to make inferences on the QAOA because of the size limitations of the instances and the lack of devices.

Table 6 aims to describe the quality of the feasible trials obtained using the quantum heuristics. Quantum circuits do not return a single answer but a series of eigenstates with corresponding frequencies. The corresponding percentage describes the likelihood of the most probable feasible solution is to be in the result of a given trial. This is unique to the success rate, as it

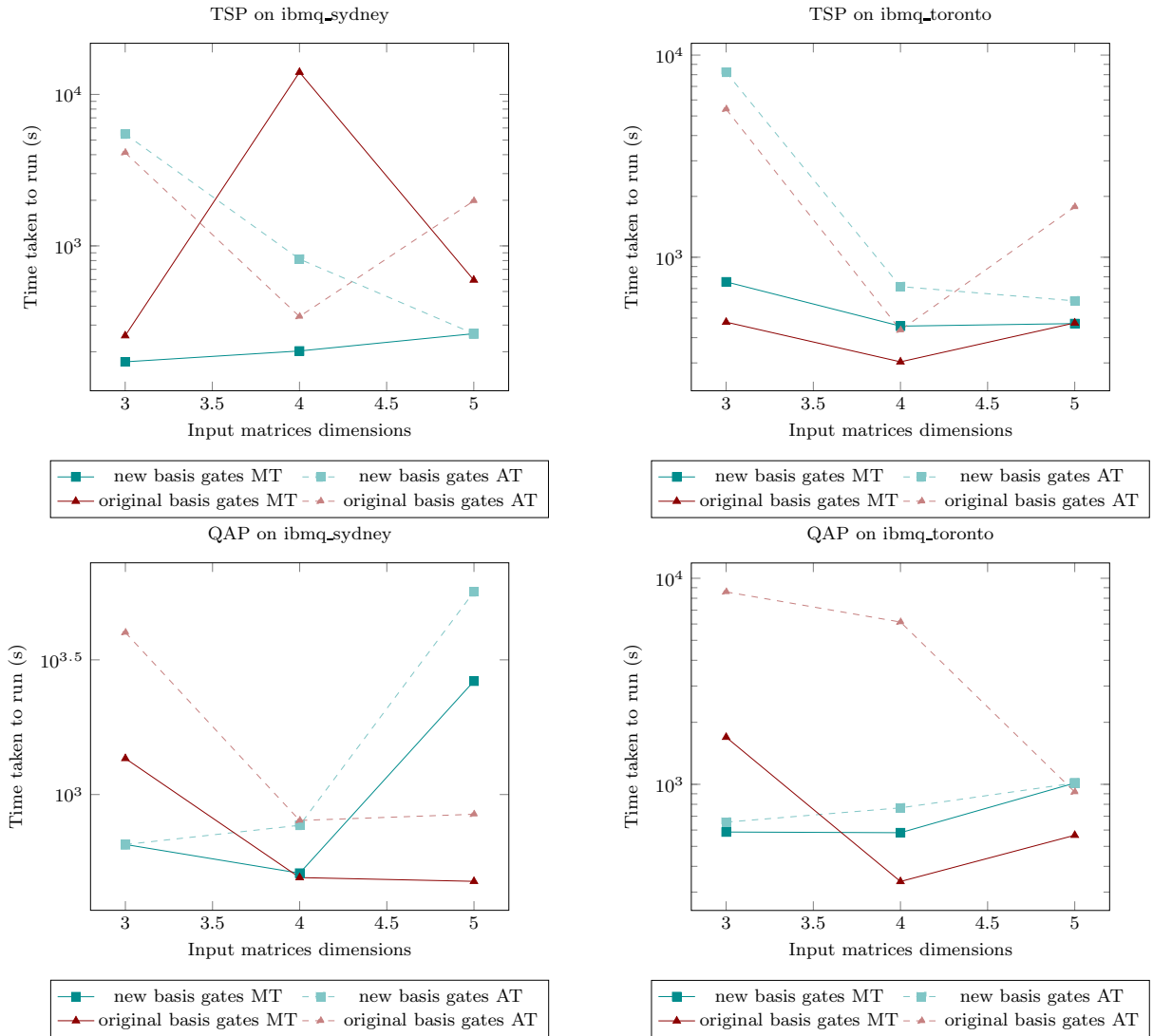


Fig. 1: These plots aim to illustrate the impact on CPU time the new set of basis gates (CX, ID, RZ, SX, X) have on ibmq_sydney and ibmq_toronto for both methods solved with VQE.

measures the uncertainty of the current trial and not the probability of success for the heuristic. This uncertainty percentage is low across all instances, indicating that most of the returned eigenstates are infeasible and highlight the detriment of noise to solution quality. This accentuates the gap in performance between simulators and the ideal solutions from theoretical quantum computers and the applied algorithms' performance on NISQ devices. There is a correlation between the size of an instance and the uncertainty percentage. Results for VQE and QAOA are comparable when comparing instances of the same size. The results obtained using the VQE algorithm with and without conditional reset are comparable when comparing instances of the same size. Conclusions about the uncertainty percentage cannot be drawn for larger problem instances, as

the set of feasible solutions is empty or singular. The NISQ devices are limited by their specifications leading to a limit in the size of the problems that can be solved. Table 2 shows the limited access to qubits that prevents the larger instances from being tested. The other specifications impact error in the results and the computational time is taken to solve circuits. Table 3 shows how the size of parameters, number of operations and circuit depth grow with problem size. This phenomenon limits experiments to small instances. Therefore, for the QAOA on both the TSP and QAP, the experiments were run until size instance 4. Instances greater than size 4 cannot be simulated in polynomial time because of the circuit depth and the number of operations produced by those instances. Obtaining a good enough initial point for instances greater than size 4 is

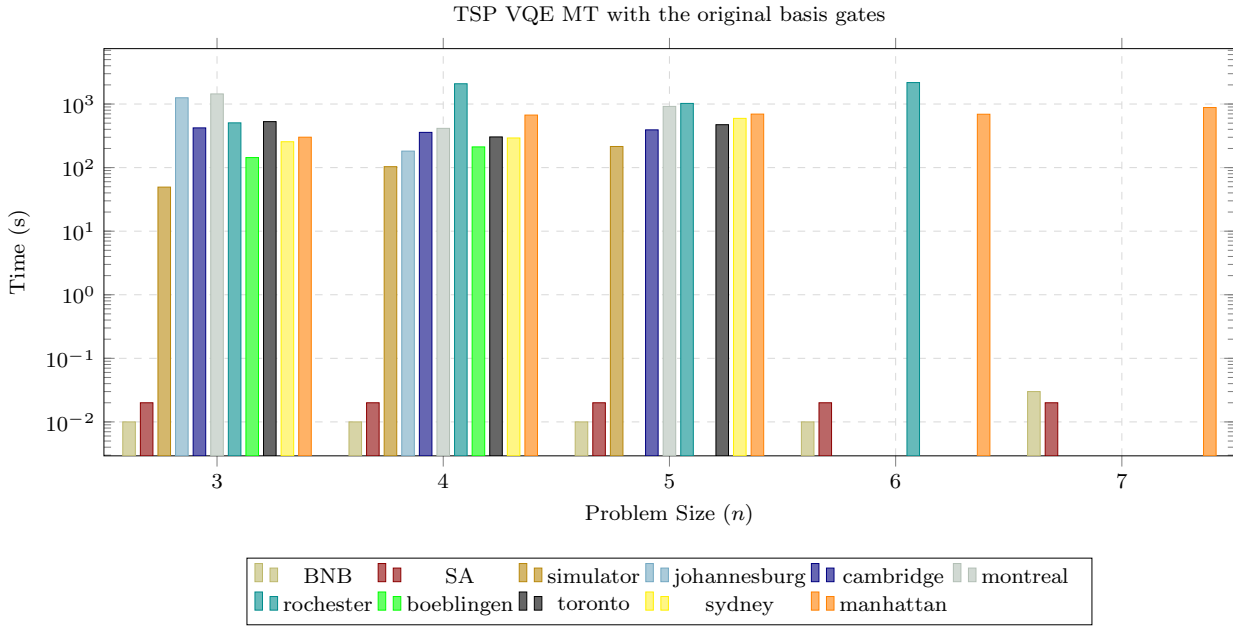


Fig. 2: CPU times (s) for TSP (Log scale)

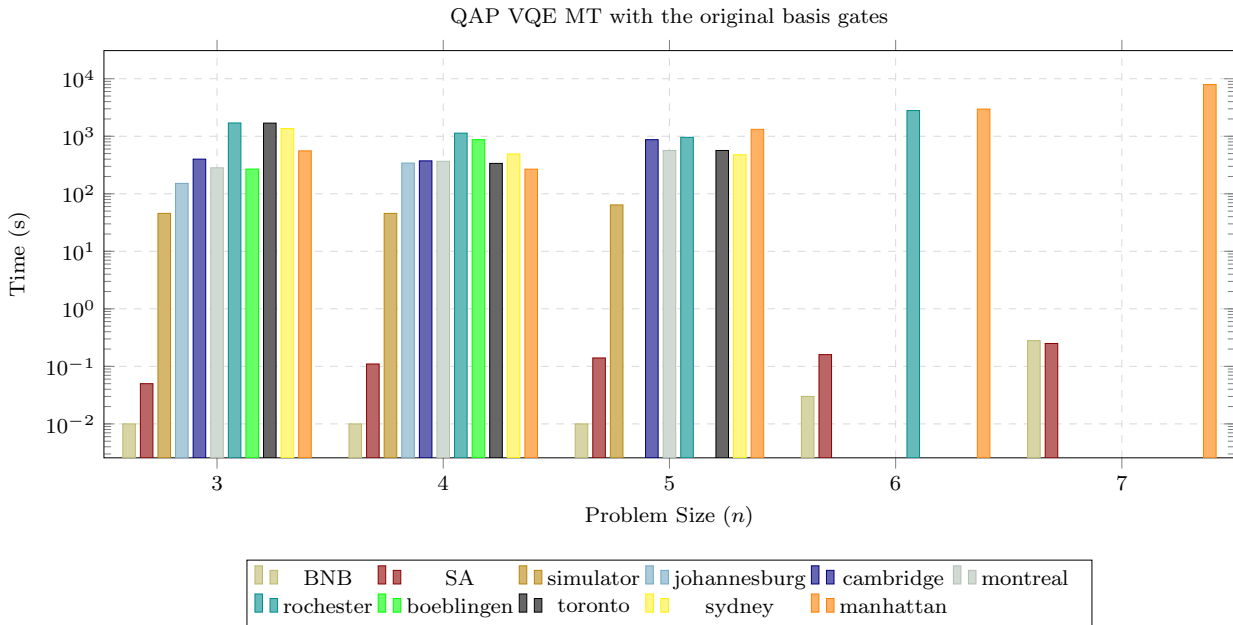


Fig. 3: CPU times (s) for QAP (Log scale)

intractable on NISQ devices. QAOA uses more operations than VQE for problems of the same size, which may impact why it performs worse than VQE on all metrics.

6 Conclusion

The results show the limitations of NISQ devices, given that the classical optimisation techniques perform sig-

nificantly better in terms of computational time, success rate, feasibility and uncertainty percentage. Furthermore, given the limited number of available qubits and limitations in circuit size - the practical use of NISQ devices in this class of problem is still in its infancy. VQE and QAOA performed similarly in terms of success rate, feasibility and uncertainty percentage. However, QAOA is limited to fewer instances and has a longer computational time than VQE. The perfor-

Table 3: Specifications of the circuits before transpiling on the quantum devices

Size	Qubits	TSP			QAP			Method
		Par. [†]	Operations	Depth	Par. [†]	Operations	Depth	
3	9	[100, "TL"]	103	23	[1000, "TL"]	103	23	VQE
		[50]	396	116	[100]	396	149	QAOA
4	16	[1100, "TL"]	187	30	[3000, "TL"]	187	30	VQE
		[100]	992	182	[50]	992	218	QAOA
5	25	[5500, "RA"]	197	33	[5000, "TL"]	295	39	VQE
		-	2000	260	-	1820	227	QAOA
6	36	[5000, "TL"]	427	50	[6000, "TL"]	427	50	VQE
		-	3528	359	-	3528	312	QAOA
7	49	[10000, "TL"]	583	63	[12000, "TL"]	583	63	VQE
		-	5684	565	-	6818	540	QAOA
8	64	-	763	78	-	763	78	VQE
		-	8576	590	-	10088	728	QAOA
9	81	-	967	95	-	967	95	VQE
		-	12312	722	-	15552	970	QAOA

[†] For VQE - [number of SPSA trials, variational form],

For QAOA - [number of SPSA trials]

Table 4: Experimental Results: quantum results with the original basis gates and all classical results

Size	TSP					QAP					Devices	Method			
	Par. [†]	SR99	SR95	Feas.*	AT(s)*	MT(s)*	Par. [†]	SR99	SR95	Feas.*	AT(s)*	MT(s)*			
3	[100, "TL"]	100.0	100.0	100.0	43.33	43.33	[1000, "TL"]	100.0	100.0	45.65	45.65	ibmq_qasm-simulator	VQE		
		100.0	100.0	100.0	2909.70	1771.32		86.67	86.67	100.0	1486.68	151.78			
		100.0	100.0	100.0	1981.35	1485.74		43.33	43.33	100.0	479.18	415.05			
		100.0	100.0	100.0	423.84	423.84		96.67	96.67	100.0	414.38	520.24			
		100.0	100.0	100.0	7271.66	1494.03		53.33	53.33	100.0	987.22	548.20			
		100.0	100.0	100.0	201.78	143.84		0.0	0.0	100.0	852.69	268.71			
		100.0	100.0	100.0	4125.49	255.25		93.33	93.33	100.0	3994.88	1360.91			
		100.0	100.0	100.0	5401.14	528.74		73.33	73.33	100.0	8586.37	1692.50			
		100.0	100.0	100.0	530.38	300.90		96.67	96.67	100.0	3722.58	557.68			
		[0.01, 10, 0.8, 10]	100.0	100.0	0.02	0.02		[1.0, 20, 0.90, 20]	100.0	100.0	0.05	0.05	classical-device	SA	
4	[1100, "TL"]	-	-	-	0.01	0.01	[3000, "TL"]	-	-	-	-	classical-device	BNB		
		3.33	3.33	73.33	54.46	54.46		0.0	100.0	100.0	45.64	45.64	ibmq_qasm-simulator	VQE	
		23.33	23.33	56.67	215.49	215.49		3.33	16.67	56.67	495.10	342.20	ibmq_johannesburg		
		13.33	13.33	53.33	681.85	445.32		3.33	6.67	56.67	827.51	369.81	ibmq_montreal		
		16.67	16.67	43.33	365.35	365.35		6.67	13.33	63.33	562.17	367.47	ibmq_cambridge		
		23.33	0.0	43.33	2006.08	1276.74		6.67	13.33	43.33	4803.45	3260.97	ibmq_rochester		
		6.67	6.67	30.0	230.62	211.68		0.0	10.0	46.67	1397.01	873.04	ibmq_boeblingen		
		3.33	3.33	6.67	341.72	292.52		0.0	3.33	36.67	801.31	491.77	ibmq_sydney		
		16.67	16.67	40.0	436.00	303.75		0.0	6.67	40.0	6133.34	337.68	ibmq_toronto		
		23.33	0.0	33.33	2487.12	670.67		0.0	10.0	40.0	298.94	267.96	ibmq_manhattan		
5	[5500, "RA"]	[0.01, 10, 0.8, 10]	100.0	100.0	100.0	0.02	0.02	[1.0, 20, 0.90, 20]	100.0	100.0	100.0	0.11	0.11	classical-device	SA
		-	-	-	0.01	0.01	[5000, "TL"]	-	-	-	-	0.01	0.01	classical-device	BNB
		26.67	26.67	26.67	99.51	92.17		0.0	0.0	96.67	64.05	64.05	ibmq_qasm-simulator	VQE	
		0.0	0.0	0.0	562.13	388.65		0.0	0.0	0.0	9986.32	872.01	ibmq_montreal		
		0.0	0.0	0.0	1135.77	439.38		0.0	0.0	0.0	565.01	565.01	ibmq_cambridge		
		3.33	3.33	3.33	13137.19	1228.91		0.0	0.0	0.0	2116.71	1801.51	ibmq_rochester		
		0.0	0.0	3.33	1982.69	594.93		0.0	0.0	0.0	845.03	476.22	ibmq_sydney		
		0.0	0.0	3.33	1774.34	473.06		3.33	3.33	6.67	917.79	566.01	ibmq_toronto		
		0.0	0.0	3.33	1836.56	694.60		0.0	0.0	3.33	3020.28	1318.44	ibmq_manhattan		
		[0.01, 10, 0.8, 10]	100.0	100.0	100.0	0.02	0.02	[1.0, 20, 0.90, 20]	100.0	100.0	100.0	0.14	0.14	classical-device	SA
6	[5000, "TL"]	-	-	-	0.01	0.01	[6000, "TL"]	-	-	-	-	0.01	0.01	classical-device	BNB
		0.0	0.0	0.0	2476.87	2176.15		0.0	0.0	3.33	5017.53	2265.98	ibmq_rochester	VQE	
		0.0	0.0	0.0	752.17	691.01		0.0	0.0	0.0	24373.16	2967.89	ibmq_manhattan		
		[0.01, 10, 0.8, 10]	100.0	100.0	100.0	0.02	0.02	[1.0, 20, 0.90, 20]	60.0	100.0	100.0	0.16	0.16	classical-device	SA
7	[10000, "TL"]	-	-	-	0.01	0.01	-	-	-	-	-	0.03	0.03	classical-device	BNB
		0.0	0.0	0.0	2525.73	881.23		[12000, "TL"]	0.0	0.0	0.0	18429.26	7928.29	ibmq_manhattan	VQE
		[0.01, 10, 0.8, 10]	66.67	66.67	100.0	0.02	0.02	[1.0, 20, 0.90, 740]	93.3	93.3	100.0	0.25	0.25	classical-device	SA
		-	-	-	-	0.03	0.03	-	-	-	0.28	0.28	classical-device	BNB	

* Feas. - percentage feasible: AT - average time with outliers, MT - average time without outliers

[†] For VQE - [number of SPSA trials, variational form],

For SA - [tolerance, Markov chain length, cooldown factor, starting temperature]

Table 5: Experimental quantum results with new basis gates

Size	TSP						QAP						Devices		Method
	Par. [†]	SR99	SR95	Feas.*	AT(s)*	MT(s)*	Par. [†]	SR99	SR95	Feas.*	AT(s)*	MT(s)*			
3	[100, “TL”]	100.0	100.0	100.0	5474.48	171.65	[1000, “TL”]	86.67	86.67	100.0	652.57	652.57	ibmq_sydney		VQE
		100.0	100.0	100.0	8226.18	477.47		30.0	30.0	100.0	655.30	586.91	ibmq_toronto		
	[50]	90.00	90.0	90.0	124.59	124.59		30.0	30.0	100.0	62.57	62.57	ibmq_qasm-simulator		QAOA
		100.0	100.0	100.0	3856.01	730.30		-	-	-	-	-	ibmq_sydney		
		100.0	100.0	100.0	10871.32	755.40		0.0	0.0	100.0	552.26	453.37	ibmq_toronto		
4	[1100, “TL”]	10.0	10.0	36.67	817.91	202.40	[3000, “TL”]	3.33	6.67	36.67	768.95	510.72	ibmq_sydney		VQE
		6.67	6.67	33.33	715.83	456.22		0.0	3.33	30.0	720.66	582.44	ibmq_toronto		
	[100]	0.0	0.0	0.0	164.05	164.05		0.0	0.0	23.33	140.96	140.96	ibmq_qasm-simulator		QAOA
		0.0	20.0	43.33	14007.94	901.45		-	-	-	-	-	ibmq_sydney		
		23.33	23.33	43.33	2325.83	1055.58		0.0	6.67	36.67	6979.90	1446.55	ibmq_toronto		
5	[5500, “RA”]	0.0	0.0	3.33	263.23	263.23	[5000, “TL”]	0.0	0.0	0.0	5659.09	2636.32	ibmq_sydney		VQE
		0.0	0.0	0.0	608.42	469.60		0.0	0.0	3.33	1014.09	1014.09	ibmq_toronto		

* Feas. - percentage feasible: AT - average time with outliers, MT - average time without outliers

† For VQE - [number of SPSA trials, variational form],

For QAOA - [number of SPSA trials]

Table 6: Experimental Results: describing the uncertainty percentage metric

Size	TSP				QAP				Devices		CR. [†]	Method	
	# feas. [†]	mean (%)	max (%)	min (%)	std (%)	# feas. [†]	mean (%)	max (%)	min (%)	std (%)			
3	30	22.36	99.41	0.10	35.35	30	95.65	98.93	0.68	17.64	ibmq_qasm-simulator	F	VQE
	30	0.70	1.75	0.29	0.35	30	0.57	1.07	0.20	0.22	ibmq_johannesburg	F	
	30	0.52	0.97	0.19	0.14	30	0.41	0.78	0.20	0.13	ibmq_montreal	F	
	30	1.14	3.03	0.20	0.96	30	2.79	4.69	0.59	1.22	ibmq_cambridge	F	
	30	0.01	0.01	0.01	0.0	30	0.55	1.07	0.20	0.21	ibmq_rochester	F	
	30	0.41	0.59	0.20	0.12	30	0.64	0.98	0.39	0.18	ibmq_boeblingen	F	
	30	0.52	0.98	0.20	0.20	30	1.04	2.54	0.20	0.48	ibmq_sydney	F	
	30	0.52	0.88	0.20	0.17	30	0.59	0.98	0.20	0.21	ibmq_toronto	F	
	30	6.02	24.51	0.20	7.27	30	28.62	35.25	0.29	5.96	ibmq_manhattan	F	
	30	0.53	1.17	0.20	0.22	30	0.77	2.05	0.20	0.43	ibmq_sydney	T	
	30	0.48	0.78	0.20	0.13	30	0.49	0.88	0.20	0.16	ibmq_toronto	T	
4	27	0.33	0.88	0.10	0.21	30	0.47	1.07	0.10	0.25	ibmq_qasm-simulator	T	QAOA
	30	0.36	0.68	0.20	0.11	-	-	-	-	-	ibmq_sydney	T	
	30	0.41	0.68	0.20	0.13	30	0.39	0.68	0.2	0.13	ibmq_toronto	T	
	22	32.51	98.63	0.10	30.83	30	96.68	98.34	48.63	8.92	ibmq_qasm-simulator	F	
	17	0.10	0.20	0.10	0.02	17	0.10	0.20	0.10	0.02	ibmq_johannesburg	F	
	16	0.10	0.10	0.10	0.0	17	0.10	0.10	0.10	0.0	ibmq_montreal	F	
	13	0.10	0.10	0.10	0.0	13	0.10	0.10	0.10	0.0	ibmq_cambridge	F	
	13	0.11	0.20	0.10	0.04	19	0.10	0.20	0.10	0.02	ibmq_rochester	F	
	9	0.10	0.10	0.10	0.0	14	0.10	0.10	0.10	0.0	ibmq_boeblingen	F	
	13	0.10	0.10	0.10	0.0	11	0.10	0.10	0.10	0.0	ibmq_sydney	F	
	12	0.10	0.10	0.10	0.10	12	0.10	0.10	0.10	0.0	ibmq_toronto	F	
	10	0.10	0.10	0.10	0.0	12	0.10	0.10	0.10	0.0	ibmq_manhattan	F	
	11	0.11	0.20	0.10	0.03	11	0.11	0.20	0.10	0.03	ibmq_sydney	T	
	10	0.10	0.10	0.10	0.0	9	0.10	0.10	0.10	0.0	ibmq_toronto	T	
5	0	-	-	-	-	7	0.10	0.10	0.10	0.0	ibmq_qasm-simulator	T	QAOA
	13	0.10	0.10	0.10	0.0	-	-	-	-	-	ibmq_sydney	T	
	13	0.10	0.10	0.10	0.0	11	0.10	0.10	0.10	0.0	ibmq_toronto	T	
	8	28.05	48.63	0.10	18.49	29	94.24	94.24	94.24	0.0	ibmq_qasm-simulator	F	
	0	-	-	-	-	0	-	-	-	-	ibmq_montreal	F	
	0	-	-	-	-	0	-	-	-	-	ibmq_cambridge	F	
	1	0.10	0.10	0.10	0.0	0	-	-	-	-	ibmq_rochester	F	
6	1	0.10	0.10	0.10	0.0	0	-	-	-	-	ibmq_sydney	F	VQE
	1	0.10	0.10	0.10	0.0	2	0.10	0.10	0.10	0.0	ibmq_toronto	F	
	1	0.10	0.10	0.10	0.0	1	0.10	0.10	0.10	0.0	ibmq_manhattan	F	
	1	0.10	0.10	0.10	0.0	0	-	-	-	-	ibmq_sydney	T	
	0	-	-	-	-	1	0.10	0.10	0.10	0.0	ibmq_toronto	T	
7	0	-	-	-	-	0	-	-	-	-	ibmq_manhattan	F	VQE
	0	-	-	-	-	0	-	-	-	-	ibmq_manhattan	F	

† # feas. - number of the 30 trials that are feasible

CR - conditional reset (T for True and F for False)

mance of NISQ devices could prospectively improve in the future as quantum technology evolves. The introduction of the conditional reset feature with new basis gates was not able to show improvement in any metrics. Importantly, however, the computational results presented herein extend and agree with other findings in the literature [45, 2, 9].

In future work, other formulations that are available such as QUBO and ADMM, could be investigated. The promise of IBM's devices with higher-performing processors and more qubits provides hope for higher quality solutions for COP.

Acknowledgement

The authors of this research paper acknowledge the University of the Witwatersrand, Johannesburg contribution through its support and Quantum Computing resources, which made this research possible. We acknowledge the use of IBM Quantum services for this work. The views expressed are those of the authors, and do not reflect the official policy or position of IBM or the IBM Quantum team.

Declarations

Funding

Not applicable.

Conflict of Interest/Competing interests

The authors declare that they have no conflict of interest.

Availability of Data and Material

The open-source data libraries used are referenced in the paper.

Code Availability

The code used to conduct this research has been made available on GitHub. Details to the repository are noted in the paper.

References

1. The Traveling Salesman Problem, pp. 527–562. Springer Berlin Heidelberg, Berlin, Heidelberg (2008). DOI 10.1007/978-3-540-71844-4_21. URL https://doi.org/10.1007/978-3-540-71844-4_21
2. Ajagekar, A., You, F.: Quantum computing for energy systems optimization: Challenges and opportunities. *Energy* **179**, 76–89 (2019)
3. Asfaw, A., Bello, L., Ben-Haim, Y., Bravyi, S., Capelluto, L., Vazquez, A.C., Ceroni, J., Harkins, F., Gambetta, J., Garion, S., Gil, L., Gonzalez, S.D.L.P., McKay, D., Minev, Z., Nation, P., Phan, A., Rattew, A., Schaefer, J., Shabani, J., Smolin, J., Temme, K., Tod, M., Wootton, J.: Learn Quantum Computation Using Qiskit (2020). URL <http://community.qiskit.org/textbook>
4. Bennett, C.H., Bernstein, E., Brassard, G., Vazirani, U.: Strengths and weaknesses of quantum computing. *SIAM journal on Computing* **26**(5), 1510–1523 (1997)
5. Bernstein, E., Vazirani, U.: Quantum complexity theory. *SIAM Journal on computing* **26**(5), 1411–1473 (1997)
6. Bland, R.G., Shallcross, D.F.: Large travelling salesman problems arising from experiments in x-ray crystallography: A preliminary report on computation. *Operations Research Letters* **8**(3), 125–128 (1989). DOI [https://doi.org/10.1016/0167-6377\(89\)90037-0](https://doi.org/10.1016/0167-6377(89)90037-0). URL <https://www.sciencedirect.com/science/article/pii/0167637789900370>
7. Burkard, R.E., Cela, E., Pardalos, P.M., Pitsoulis, L.S.: The quadratic assignment problem. In: *Handbook of combinatorial optimization*, pp. 1713–1809. Springer (1998)
8. Burkard, R.E., Offermann, J.: Entwurf von schreibmaschinentastaturen mittels quadratischer zuordnungsprobleme. *Zeitschrift für Operations Research* **21**(4), B121–B132 (1977)
9. Chieza, H., Khumalo, M., Prag, K., Woolway, M.: On the computational performance of ibm quantum devices applied to combinatorial optimisation problems. In: 2020 7th International Conference on Soft Computing & Machine Intelligence (ISCMI), pp. 260–264. IEEE (2020)
10. Clausen, J.: Branch and bound algorithms-principles and examples (1999)
11. Crooks, G.E.: Performance of the quantum approximate optimization algorithm on the maximum cut problem. *arXiv preprint arXiv:1811.08419* (2018)
12. Dantzig, G.B., Fulkerson, D.R., Johnson, S.M.: On a linear-programming, combinatorial approach to the traveling-salesman problem. *Operations Research* **7**(1), 58–66 (1959). URL <http://www.jstor.org/stable/167593>
13. Dantzig, G.B., Ramser, J.H.: The truck dispatching problem. *Management science* **6**(1), 80–91 (1959)
14. Deutsch, D.: Quantum theory, the church-turing principle and the universal quantum computer. *Proceedings of the Royal Society of London. A. Mathematical and Physical Sciences* **400**(1818), 97–117 (1985)
15. Dickey, J., Hopkins, J.: Campus building arrangement using topaz. *Transportation Research* **6**(1), 59–68 (1972)
16. Dorigo, M., Birattari, M., Stutzle, T.: Ant colony optimization. *IEEE computational intelligence magazine* **1**(4), 28–39 (2006)
17. Elshafei, A.N.: Hospital layout as a quadratic assignment problem. *Journal of the Operational Research Society* **28**(1), 167–179 (1977)
18. Farhi, E., Gamarnik, D., Gutmann, S.: The quantum approximate optimization algorithm needs to see the whole graph: a typical case. *arXiv preprint arXiv:2004.09002* (2020)
19. Farhi, E., Goldstone, J., Gutmann, S.: A quantum approximate optimization algorithm. *arXiv preprint arXiv:1411.4028* (2014)
20. Farhi, E., Goldstone, J., Gutmann, S., Neven, H.: Quantum algorithms for fixed qubit architectures. *arXiv preprint arXiv:1703.06199* (2017)

21. Ferreira, C.: Gene expression programming: a new adaptive algorithm for solving problems. arXiv preprint cs/0102027 (2001)
22. Gavett, J.W., Plyter, N.V.: The optimal assignment of facilities to locations by branch and bound. *Operations Research* **14**(2), 210–232 (1966)
23. Grant, E., Wossnig, L., Ostaszewski, M., Benedetti, M.: An initialization strategy for addressing barren plateaus in parametrized quantum circuits. *Quantum* **3**, 214 (2019)
24. Grover, L.K.: Quantum mechanics helps in searching for a needle in a haystack. *Physical review letters* **79**(2), 325 (1997)
25. Harrigan, M.P., Sung, K.J., Neeley, M., Satzinger, K.J., Arute, F., Arya, K., Atalaya, J., Bardin, J.C., Barends, R., Boixo, S., et al.: Quantum approximate optimization of non-planar graph problems on a planar superconducting processor. *Nature Physics* pp. 1–5 (2021)
26. Hastings, W.K.: Monte carlo sampling methods using markov chains and their applications (1970)
27. Kirkpatrick, S., Gelatt, C.D., Vecchi, M.P.: Optimization by simulated annealing. *science* **220**(4598), 671–680 (1983)
28. Koopmans, T.C., Beckmann, M.: Assignment problems and the location of economic activities. *Econometrica* **25**(1), 53–76 (1957). URL <http://www.jstor.org/stable/1907742>
29. Land, A.H., Doig, A.G.: An automatic method for solving discrete programming problems. In: 50 Years of Integer Programming 1958–2008, pp. 105–132. Springer (2010)
30. Laporte, G.: The traveling salesman problem: An overview of exact and approximate algorithms. *European Journal of Operational Research* **59**(2), 231–247 (1992)
31. Lawler, E.L.: The quadratic assignment problem. *Management science* **9**(4), 586–599 (1963)
32. Lenstra, J.K., Kan, A.R.: Some simple applications of the travelling salesman problem. *Journal of the Operational Research Society* **26**(4), 717–733 (1975)
33. Lin, S., Kernighan, B.W.: An effective heuristic algorithm for the traveling-salesman problem. *Operations research* **21**(2), 498–516 (1973)
34. Lucas, A.: Ising formulations of many np problems. *Frontiers in Physics* **2**, 5 (2014)
35. McClean, J.R., Boixo, S., Smelyanskiy, V.N., Babbush, R., Neven, H.: Barren plateaus in quantum neural network training landscapes. *Nature communications* **9**(1), 1–6 (2018)
36. Metropolis, N., Rosenbluth, A.W., Rosenbluth, M.N., Teller, A.H., Teller, E.: Equation of state calculations by fast computing machines. *The journal of chemical physics* **21**(6), 1087–1092 (1953)
37. Moll, N., Barkoutsos, P., Bishop, L.S., Chow, J.M., Cross, A., Egger, D.J., Filipp, S., Fuhrer, A., Gambetta, J.M., Ganzhorn, M., et al.: Quantum optimization using variational algorithms on near-term quantum devices. *Quantum Science and Technology* **3**(3), 030503 (2018)
38. Montanaro, A.: Quantum algorithms: an overview. *npj Quantum Information* **2**(1), 1–8 (2016)
39. Morrison, D.R., Jacobson, S.H., Sauppe, J.J., Sewell, E.C.: Branch-and-bound algorithms: A survey of recent advances in searching, branching, and pruning. *Discrete Optimization* **19**, 79 – 102 (2016). DOI <https://doi.org/10.1016/j.disopt.2016.01.005>. URL <http://www.sciencedirect.com/science/article/pii/S1572528616000062>
40. Murali, P., Baker, J.M., Javadi-Abhari, A., Chong, F.T., Martonosi, M.: Noise-adaptive compiler mappings for noisy intermediate-scale quantum computers. In: Proceedings of the Twenty-Fourth International Conference on Architectural Support for Programming Languages and Operating Systems, pp. 1015–1029 (2019)
41. Peruzzo, A., McClean, J., Shadbolt, P., Yung, M.H., Zhou, X.Q., Love, P.J., Aspuru-Guzik, A., O'brien, J.L.: A variational eigenvalue solver on a photonic quantum processor. *Nature communications* **5**, 4213 (2014)
42. Rattew, A.G., Hu, S., Pistoia, M., Chen, R., Wood, S.P.: A domain-agnostic, noise-resistant, hardware-efficient evolutionary variational quantum eigensolver. arXiv: Quantum Physics (2019)
43. Rønnow, T.F., Wang, Z., Job, J., Boixo, S., Isakov, S.V., Wecker, D., Martinis, J.M., Lidar, D.A., Troyer, M.: Defining and detecting quantum speedup. *Science* **345**(6195), 420–424 (2014)
44. Sahni, S., Gonzalez, T.: P-complete approximation problems. *Journal of the ACM (JACM)* **23**(3), 555–565 (1976)
45. Srinivasan, K., Satyajit, S., Behera, B.K., Panigrahi, P.K.: Efficient quantum algorithm for solving travelling salesman problem: An ibm quantum experience. arXiv preprint arXiv:1805.10928 (2018)
46. Streif, M., Leib, M.: Training the quantum approximate optimization algorithm without access to a quantum processing unit. *Quantum Science and Technology* **5**(3), 034008 (2020)
47. Stützle, T.: Max-min ant system for quadratic assignment problems (1997)
48. Taillard, É.: Robust taboo search for the quadratic assignment problem. *Parallel computing* **17**(4-5), 443–455 (1991)
49. Van Laarhoven, P.J., Aarts, E.H.: Simulated annealing. In: *Simulated annealing: Theory and applications*, pp. 7–15. Springer (1987)
50. Verteletskyi, V., Yen, T.C., Izmaylov, A.F.: Measurement optimization in the variational quantum eigensolver using a minimum clique cover. *The Journal of chemical physics* **152**(12), 124114 (2020)
51. Warren, R.H.: Small traveling salesman problems. *Journal of Advances in Applied Mathematics* **2**(2) (2017)
52. Wilhelm, M.R., Ward, T.L.: Solving quadratic assignment problems by ‘simulated annealing’. *IIE transactions* **19**(1), 107–119 (1987)
53. Willsch, M., Willsch, D., Jin, F., De Raedt, H., Michielsen, K.: Benchmarking the quantum approximate optimization algorithm. *Quantum Information Processing* **19**, 1–24 (2020)
54. Zahedinejad, E., Zaribafyan, A.: Combinatorial optimization on gate model quantum computers: A survey. arXiv preprint arXiv:1708.05294 (2017)
55. Zhou, A.H., Zhu, L.P., Hu, B., Deng, S., Song, Y., Qiu, H., Pan, S.: Traveling-salesman-problem algorithm based on simulated annealing and gene-expression programming. *Information* **10**(1), 7 (2019)
56. Zhou, L., Wang, S.T., Choi, S., Pichler, H., Lukin, M.D.: Quantum approximate optimization algorithm: Performance, mechanism, and implementation on near-term devices. *Physical Review X* **10**(2), 021067 (2020)